

# High Precision CTE-Measurement of SiC-100 for Cryogenic Space-Telescopes

K. Enya<sup>1</sup>, N. Yamada<sup>2</sup>, T. Onaka<sup>3</sup>, T. Nakagawa<sup>1</sup>, H. Kaneda<sup>1</sup>, M. Hirabayashi<sup>4</sup>,  
Y. Toulemont<sup>5</sup>, D. Castel<sup>5</sup>, Y. Kanai<sup>6</sup>, and N. Fujishiro<sup>6</sup>

enya@ir.isas.jaxa.jp

Received \_\_\_\_\_; accepted \_\_\_\_\_

---

<sup>1</sup> Institute of Space and Astronautical Science, Japan Aerospace Exploration Agency, 3-1-1 Yoshinodai, Sagami-hara, Kanagawa 229-8510, Japan

<sup>2</sup> National Metrology Institute of Japan, Advanced Industrial Science and Technology, 3 Tsukuba Central, Tsukuba, Ibaraki 305-8563, Japan

<sup>3</sup> Department of Astronomy, Graduate School of Science, University of Tokyo, 7-3-1 Hongo, Bunkyo-ku, Tokyo 113-0033, Japan

<sup>4</sup> Sumitomo Heavy Industries, Ltd., 5-2 Niihama Works, Soubiraki-cho, Niihama, Ehime 792-9599, Japan

<sup>5</sup> Astrium Satellites, Earth Observation, Navigation & Science (F), 31 av des Cosmonautes, 31042 Toulouse Cedex 4, France

<sup>6</sup> Genesia Corporation, Mitaka Sangyo Plaza 601, 3-38-4 Shimorenjyaku, Mitaka, Tokyo 181-0013, Japan

## ABSTRACT

We present the results of high precision measurements of the thermal expansion of the sintered SiC, SiC-100, intended for use in cryogenic space-telescopes, in which minimization of thermal deformation of the mirror is critical and precise information of the thermal expansion is needed for the telescope design. The temperature range of the measurements extends from room temperature down to  $\sim 10$  K. Three samples, #1, #2, and #3 were manufactured from blocks of SiC produced in different lots. The thermal expansion of the samples was measured with a cryogenic dilatometer, consisting of a laser interferometer, a cryostat, and a mechanical cooler. The typical thermal expansion curve is presented using the 8th order polynomial of the temperature. For the three samples, the coefficients of thermal expansion (CTE),  $\bar{\alpha}_{\#1}$ ,  $\bar{\alpha}_{\#2}$ , and  $\bar{\alpha}_{\#3}$  were derived for temperatures between 293 K and 10 K. The average and the dispersion ( $1\sigma$  rms) of these three CTEs are 0.816 and  $0.002 (\times 10^{-6}/\text{K})$ , respectively. No significant difference was detected in the CTE of the three samples from the different lots. Neither inhomogeneity nor anisotropy of the CTE was observed. Based on the obtained CTE dispersion, we performed an finite-element-method (FEM) analysis of the thermal deformation of a 3.5 m diameter cryogenic mirror made of six SiC-100 segments. It was shown that the present CTE measurement has a sufficient accuracy well enough for the design of the 3.5 m cryogenic infrared telescope mission, the Space Infrared telescope for Cosmology and Astrophysics (SPICA).

*Subject headings:* instrumentation: miscellaneous — methods: laboratory — techniques: miscellaneous

## 1. Introduction

Development of cryogenic light-weight mirrors is a key technology for infrared astronomical space-telescope missions, which have large advantages owing to being free from the turbulence, thermal background, and absorption caused by atmosphere. The light-weight mirror technology is essential to bring large mirrors into space that enable a high sensitivity and a high spatial resolution. The infrared sensitivity of the space-telescope is vastly improved by reduction of the thermal background by cooling the telescope to cryogenic temperatures. Thus infrared space telescopes badly need cooled light-weight mirrors with a sufficient optical quality.

Silicon-carbide (SiC) is one of the most promising materials for space telescopes because of its high ratio of stiffness to density. Japanese space mission for infrared astronomy, *AKARI*, carries a 68.5 cm aperture telescope whose mirrors are made of sandwich type SiC (Murakami 2004; Kaneda et al. 2005). The entire *AKARI* telescope system is cooled down to 6 K by helium gas vaporizing from liquid helium. *AKARI* was launched in February 2006 and the telescope system performance has been confirmed to be as expected from pre-launch ground tests (Kaneda et al. 2007). The Herschel Space Observatory, a submillimeter satellite mission by the European Space Agency (Pilbratt 2004), employs mirrors of sintered SiC (SiC-100) provided by Boostec Industries and EADS-Astrium (Breyse et al. 2004). The 3.5m diameter primary mirror of the Herschel telescope is made of 12 segments brazed together. The Herschel Space Observatory will be launched in 2008 to make observations in 60–670  $\mu\text{m}$ , whilst the telescope will be kept to  $\sim 80$  K by passive cooling. SiC-100 is one of the most frequently used SiCs for space optics. It has been used for the telescopes of ALADIN, GAIA, ROCSAT and other missions (Breyse et al. 2004 and the references therein).

The Space Infrared telescope for Cosmology and Astrophysics (SPICA) is the next

generation mission for infrared astronomy, planned by the Japan Aerospace Exploration Agency (Nakagawa 2004; Onaka et al. 2005). The SPICA telescope is required to have a 3.5 m diameter aperture and will be cooled down to 4.5 K by the combination of radiative cooling and mechanical coolers (Sugita et al. 2006). SPICA is planned to be launched in the middle of the 2010s and execute infrared observations in 5–200  $\mu\text{m}$ . SiC-100 is one of the promising candidate materials for the mirrors and structures of the SPICA telescope, whilst carbon-fiber reinforced silicon-carbide is another candidate now being investigated (Ozaki et al. 2004; Enya et al. 2006; Enya et al. 2004). Monolithic primary mirrors can be manufactured by the joint segment technology, similar to the primary mirror for the Herschel telescope. The requirement for the surface figure accuracy of the SPICA primary mirror is, however, better than 0.06  $\mu\text{m}$  rms. This requirement is  $\sim 20$  times more severe than the Herschel Space Observatory because of the difference in the targeted wavelength range.

In the development of cryogenic space-telescopes, it is important to suppress the thermal deformation of the mirror caused by cooling to satisfy the requirement for the surface figure accuracy (Kaneda et al. 2003; Kaneda et al. 2005). Therefore, the study of the coefficients of thermal expansion (CTE) of the material used for the mirror is important. The CTE data of the mirror material are indispensable for the design of cryogenic space-telescopes because the actual telescope mirror needs to accommodate complicated support structures consisting of materials different from the mirror. If the CTE measurement of test pieces of the mirror material has a sufficient accuracy, it will enable us to predict the thermal deformation of a segmented mirror caused by the dispersion in the CTE of each segment. The most direct and highly sensitive test of the thermal deformation is an interferometer measurement of the actual mirror at cold temperatures. The CTE data are useful to interpret the result of direct measurements of the mirror and investigate the origin of the observed deformation.

However, measurements of the CTE of SiC and its dispersion have not so far been performed with a sufficient accuracy and for a wide temperature range. Especially, little data are available at temperatures lower than 77 K, which can be realized by only liquid nitrogen cooling. Prior to this work, available CTE data of SiC-100 were limited at temperatures higher than  $\sim 77$  K (Toulemont 2005). Pepi & Altshuler (1995) presented the CTE data of reaction bonded optical grade (RBO) SiC down to 4 K based on measurements with samples made from one block of the RBO SiC. The CTE of the new-technology SiC (NT-SiC), developed high-strength reaction-sintered SiC, has been reported down to 20 K for one sample by Suyama et al. (2005).

In this work, we present the results of high precision CTE measurements of SiC-100 down to cryogenic temperatures for samples from three different lots. We set two major goals for the present work: one is to provide the typical CTE of SiC-100 for the development of the SPICA telescope, and the other is to estimate the thermal deformation of segmented mirrors from the measured CTEs.

## 2. Experiment

### 2.1. Sample

Figure 1 shows three samples (#1, #2, and #3) of SiC-100 measured in this work. All of the samples were manufactured by Boostec Industries and EADS-Astrium (Breysse et al. 2004). Each of the samples was extracted from blocks of SiC produced in different lots. The locations of each sample in the SiC blocks are arbitrary. The samples are of a rectangular parallelepiped shape with the dimension of  $20.00^{+0.05}_{-0.00}$  mm  $\times$   $20.00^{+0.05}_{-0.00}$  mm  $\times$   $6.0^{+0.1}_{-0.0}$  mm. Flatness, parallelism, and roughness of the  $20.00$  mm  $\times$   $6.00$  mm surfaces are important for the measurement of this work: The flatness

of these surfaces is  $\leq \lambda/10$  rms, where  $\lambda$  is the wavelength of the He-Ne laser, 632.8 nm. The parallelism of the opposing 20.00 mm  $\times$  6.00 mm surfaces is less than 2'', whilst the parallelism of the opposing 20.00 mm  $\times$  20.00 mm surfaces is less than 1.0°. All of the 20.00 mm  $\times$  6.00 mm surfaces are polished to an optical grade and the surface roughness finally achieved is less than 3 nm rms. Owing to the polished surface, the directly reflected laser light by the sample was used for the measurement. As the result, the measurement was free from the uncertainty due to any additional mirrors or coating, which would be needed if the direct reflected light could not be used.

## 2.2. Measurement

The measurement of the thermal expansion was carried out with the laser interferometric dilatometer system for low temperature developed in the National Metrology Institute of Japan, Advance Industrial Science and Technology (Yamada & Okaji 2000, hereafter the paper-I; Okaji & Yamada 1997; Okaji et al. 1997). The system consists of the cryostat, the cryogenic mechanical refrigerator of the GM cycle (V204SC) by Daikin Industries Ltd., and the interferometer utilizing acousto-optical modulators and the stabilized He-Ne laser system (05STP905) by Melles Griot. The cooling is performed with the refrigerator alone and no cryogen is needed. The minimum temperature achieved in this work is about 10 K. The space around the cold stage of the cryostat, containing the installed sample, is filled with 130 Pa helium gas and sealed off at room temperature before cooling to ensure thermal uniformity. The configuration of the whole cryostat and the sample installation into the cold stage of the cryostat are shown in figures 1 and 2 of the paper-I, respectively. The change of length of the sample,  $\Delta L$ , is measured with the double path type laser interferometer of the optical heterodyne method with the digital lock-in amplifier (Model SR-850) from Stanford Research System. Details of this system are given in the paper-I.

We made totally 6 measurements of the CTEs of SiC-100. In each measurement, the sample was initially cooled down to  $\sim 10$  K and then the proportional integral derivative (PID) temperature control was applied. After the the temperature had been stabilized, the temperature and the change of the sample length  $\Delta L$  were measured. The temperature stability during the measurement was less than 0.02 K per hour. This process was repeated at approximately 16 temperatures of roughly equal intervals up to room temperature. One dataset of the temperature vs.  $\Delta L$  was obtained for one cooling cycle. To compensate the systematic uncertainty, each measurement was repeated by rotating the sample by  $90^\circ$  as described in figure 2 of the paper–I. We measured CTEs of two orthogonal directions (A and B directions as shown in figure 1) of each sample. The directions A and B were arbitrary chosen.

### 3. Result and discussion

#### 3.1. Typical thermal expansion

The results of the measurement of the thermal expansion are presented in figure 2. A fit with the 8th order polynomial is applied to each of the six datasets and the thermal expansion (contraction)  $\Delta L/L$  is set as 0 at 293 K for each of the six curves. The six datasets are plotted in figure 2 (a). We present the curve derived from the fit with all of the six datasets as the typical thermal contraction of SiC-100. It is shown by the solid line in figure 2 (a). The coefficients of the 8th order polynomial,  $\Delta L/L = \sum_{i=0}^8 a_i T^i$ , are presented in table 1. Figure 2 (b) shows the residual dispersion of the data after subtracting the fit curve. The shape of the curve in figure 2 (a) is roughly compatible with those of the RBO SiC (Pepi & Altshuler 1995) and NT-SiC (Suyama et al. 2005), though slightly negative CTEs observed in the RBO SiC and NT-SiC observed at temperatures less than 50 K are not seen in the present measurements for SiC-100. Because of the uncertainties in the other

measurements, it is difficult to further investigate the origins of the differences at present.

For each of the six curves, the average  $\Delta L/L$  per temperature between 293 K and 10 K is derived and summarized in table 2. The average of the six values and their dispersion ( $1\sigma$ ) are 0.816 and  $0.005 (\times 10^{-6}/\text{K})$ , respectively. The dispersion is smaller than the previous upper-limit obtained with high-purity single crystal silicon in paper-I,  $0.01 (\times 10^{-6}/\text{K})$ , indicating that the present measurements have reached the limit set by the instrument.

Pepi & Altshuler (1995) have shown the  $1\sigma$  dispersion of  $0.04 (\times 10^{-6}/\text{K})$  for their measurements. Karlmann et al. (2006) presented the repeatability of the CTE measurement to be  $0.004 (\times 10^{-6}/\text{K})$  from 35 K to 305 K of single crystal silicon by the interferometer based cryogenic dilatometer. Comparing with Karlmann et al. (2006), our measurement reached lower temperatures. Thus the present dispersion is concluded to be well below the measurement uncertainty and we do not detect any significant variations in the CTEs of the present 6 measurements. We do not detect either any differences in the CTEs in different directions of the same sample or any differences in the samples extracted from different lots. Thus SiC-100 we have measured is homogeneous and isotropic within the present measurement uncertainty. Finally, we average two  $\bar{\alpha}$  in directions A and B of each of three samples to obtain  $\bar{\alpha}_{\#1} = 0.8145$ ,  $\bar{\alpha}_{\#2} = 0.8160$ , and  $\bar{\alpha}_{\#3} = 0.8185 (\times 10^{-6}/\text{K})$ . The average and the dispersion ( $1\sigma$  rms) of these three CTEs are 0.816 and  $0.002 (\times 10^{-6}/\text{K})$ , respectively.

### 3.2. Alternative measurements of the dispersion of CTE

Differential tests of the CTE dispersion is another strong tool to investigate the variations in the CTEs. The quite small dispersion in the CTEs of SiC-100 has been confirmed by the systematic check made by Astrium in the manufacturing process of the

mirror segments of the Herschel Space Observatory. All the 12 segments of the Herschel primary mirror came from different SiC powder batches. The measurement of the bending deflection was made for a brazed couple of two thin SiC samples coming from different batches of SiC. The couples were placed in a vacuum chamber and the thermal deformation of the surface figure of the samples was measured by an interferometer between room temperature and 150K. The deformation data is directly linked to the curvature of the bending deflection and to the difference of the CTE between the two samples.

In order to validate the sufficient homogeneity of the SiC material, two kinds of verification on the material have been performed: One of the tests was of homogeneity inside one spare segment. For this test, samples were cut out from one spare sintered segment at several locations (along radial, tangent, and thickness directions). The other test was of homogeneity between samples belonging to different flight segments. For this test, as it was not possible to take samples from the flight segments after sintering, the samples were cut out from different segments at their green body stage, before the sintering of the segments. Those samples were taken from arbitrary locations of the segments (different orientations and locations were therefore present in the test samples). Those samples were made similar to the segments themselves by taking care of sintering them in the same run as the associated segments. By this way, it was possible to reproduce the differential CTE characteristics. In the telescope manufacturing process, 12 samples of the 12 segments were brazed on the reference samples and tested at 150K. The results indicate the dispersion ( $1\sigma$  rms) to be smaller than  $0.0025 (\times 10^{-6}/\text{K})$ .

The agreement of the dispersion of the CTE derived by two different methods signifies that both of the measurements are reliable and the uniformity of the CTE of the SiC-100 is well confirmed. The direct measurement of the CTE of this work and the differential measurement are complementary: the direct measurement provides absolute CTE data

down to 10 K with high accuracy, which is indispensable to design the space telescope including the surrounding structures, whilst the differential test checks the uniformity of the CTE for a large number of the samples.

### 3.3. Simulation of the mirror deformation

It is fruitful to relate the accuracy of the CTE measurement with corresponding thermal deformation of the mirror. In this section the thermal deformation of the segmented mirror is estimated on the basis of the measured dispersion of the CTE values. To examine this issue, we perform a case study by using a simple model of the finite-element-method (FEM) analysis. All of the simulated thermal deformation is derived for the case of cooling down from 293 K to 10 K. Figure 3 shows the model used in the FEM analysis. One mirror with a center hole is constructed from six segments with the rib structure as shown in figures 3 (a) and b as a light-weight mirror design. In this model, it was assumed that the mirror surface is flat for simplicity. Figures 3 (c) and d show a three-dimensional view and the geometry of one segment, respectively. The diameter of the whole mirror is 3.5 m, equating to the designed diameter of the primary mirror of the SPICA telescope and the Herschel Space Observatory. The thicknesses of the rib structure and mirror surface are 3 mm. The Young's modulus and Poisson's ratio of SiC-100 at room temperature are reported to be 420 GPa and 0.17, respectively (Breysse et al. 2004; Toulemont 2005). We use these values in the simulation of the thermal deformation since the temperature dependence of these quantities is usually small and not available at present. In the FEM analysis, the rotationally symmetric axis of the mirror is set along the z axis of the Cartesian coordinates. The constraints of the model are shown in figure 3 (b): Three points on the rib of the mirror, indicated by triangles, are constrained on the lines in the x-y plane as shown by the arrows in figure 3 (b). These points are free along the radial direction within the constraint

lines. Therefore, this constraints cause no inner stress in the mirror in the simulation of the cooling and thermal deformation.

The results of the simulation are presented in figure 4. Figure 4 (a) shows the thermal deformation toward the  $z$ -direction of the mirror surface obtained from the FEM analysis, in which  $\bar{\alpha}_{\#1}$ ,  $\bar{\alpha}_{\#2}$ , and  $\bar{\alpha}_{\#3}$  are given for the segment s5 and s6, s1 and s2, s3 and s4, respectively (case-I). Figure 4 (b) shows the simulated  $z$ -direction deformation, in which  $\bar{\alpha}_{\#1}$ ,  $\bar{\alpha}_{\#2}$ , and  $\bar{\alpha}_{\#3}$  were given for the segment s3 and s6, s2 and s5, s1 and s4, respectively (case-II). The case-I and case-II are the configuration, in which the two segments having the same CTE are allocated to be adjoined and confronted position, respectively. As the result, the configuration of the case-I corresponds to a mirror, which consists of three segments having  $\bar{\alpha}_{\#1}$ ,  $\bar{\alpha}_{\#2}$ , and  $\bar{\alpha}_{\#3}$ , whilst the configuration of the case-II corresponds to a mirror having a CTE distribution of  $180^\circ$  rotationally symmetric. Both of figures 4 (a) and (b) show the surface after the tilt correction. For the case-I and case-II,  $0.032 \mu\text{m}$  and  $0.040 \mu\text{m}$  ( $1 \sigma$  rms) are obtained as the surface deformation after the tilt correction, respectively. Since the requirement for the surface figure accuracy of SPICA is  $0.06 \mu\text{m}$  rms, the FEM analysis indicates that the thermal deformation estimated based on the measured CTE dispersion among the segments is sufficiently small for the SPICA telescope.

The temperature expected for the SPICA is 4.5 K, whilst the lowest temperature of the CTE measurement in this work is  $\sim 10$  K. However, the thermal contraction between 10 K and 4.5 K is negligible and does not affect the mirror deformation at all. It is shown that the accuracy of the CTE measurement achieved in the present study is sufficient to investigate the thermal deformation for the wave front error of less than  $0.06 \mu\text{m}$  for a segmented SiC mirror of 3.5m size.

#### 4. Conclusion

In this work, we performed high precision measurement of the thermal expansion of the sintered SiC, SiC-100 for use in cryogenic space-telescopes. Three samples of SiC-100 from different lots are measured. The temperature the measurement ranges from room temperature to  $\sim 10$  K. The following results are obtained.

1. The typical thermal expansion of SiC-100 is given in the form of  $\Delta L/L = \sum_{i=0}^8 a_i T^i$ . The coefficients are shown in table 1.
2. The CTEs were measured for three samples of two orthogonal directions., The average and dispersion ( $1\sigma$ ) of these six values between 293 K and 10 K are 0.816 and 0.005 ( $10^{-6}/\text{K}$ ), respectively. The dispersion is well below the present measurement uncertainty.
3. The homogeneity and the anisotropy of the CTE of SiC-100 has been confirmed within the present measurement accuracy.
4. The small dispersion of the absolute CTE obtained is compatible with the results of the differential CTE measurements using brazed samples made at Astrium.
5. For the three samples, nominal CTEs,  $\bar{\alpha}_{\#1}$ ,  $\bar{\alpha}_{\#2}$ , and  $\bar{\alpha}_{\#3}$  were derived for temperatures between 293 K and 10 K by averaging two CTE data of tow directions for each sample.
6. The thermal deformation of a segmented mirror is estimated by a FEM analysis, using  $\bar{\alpha}_{\#1}$ ,  $\bar{\alpha}_{\#2}$ , and  $\bar{\alpha}_{\#3}$ . The result indicates that the present measured dispersion is sufficiently small and well below the SPICA requirement on thermal deformation of the mirror, 0.06  $\mu\text{m}$  rms.

We are grateful for Dr. Masahiro Okaji in National Metrology Institute of Japan, Advance Industrial Science and Technology for kind and large support for the measurement. This work was supported in part by a grant from the Japan Science and Technology Agency.

## REFERENCES

- Breysse, J., Castel, D., Laviron, B., Logut, D., & Bougoin, M., 2004, Proc. of the 5th International Conference on Space Optics, 659
- Enya, K., Nakagawa, T., Kataza, H., Kaneda, H., Y.Y.Yamashita, T. Onaka, T. Oshima, & T. Ozaki, 2004, Proc. of SPIE, 5487, 1092
- Enya, K., Nakagawa, T., Kaneda, H., Onaka, T., Ozaki, T., & Kume, M., 2007, Applied Optics, in press
- Kaneda, H., Onaka, T., Yamashiro, R., & Nakagawa, T., 2003, Proc. of SPIE, 4850, 230
- Kaneda, H., Onaka, T., Nakagawa, T., Enya, K., Murakami, H., Yamashiro, R., Ezaki, T., Numao, Y., & Sugiyama, Y., 2005, Applied Optics, 44, 6823
- Kaneda, H., Kim, W., Onaka, T., Wada, T., Ita, Y., Sakon, I., & Takagi, T., 2007, Publ. Astron. Soc. Japan, submitted
- Karlmann, P. B., Klein, K. J., Halverson, P. G., Peters, R. D., Levine, M. B., van Buren, D., & Dudik, M. J., 2006, Proc. of AIP Conferenc, Advances in Cryogenic Engineering, 824, 35
- Murakami, H., 2004, Proc. of SPIE, 5487, 330
- Nakagawa, T., & SPICA working group, 2004, Adv. Sp. Res., 34, 645
- Okaji, M., & Yamada, N., 1997, High Temp. & High Press., 29, 89
- Okaji, M., Yamada, N., Kato, H., & Nara, H., 1997, Cryogenics, 37, 251
- Onaka, T., Kaneda, H., Enya, K., Nakawaga, T., Murakami, H., Matsuhara, H., & Kataza, H., 2005, Proc. of SPIE, 5494, 448

- Ozaki, T., Kume, M., Oshima, T., Nakagawa, T., Matsumoto, T., Kaneda, H., Murakami, H., Kataza, H., Enya, K., T. Onaka, & M. Krodel, 2004, Proc. of SPIE, 5494, 366
- Sugita, H., Nakagawa, T., Murakami, H., Okamoto, A., Nagai, H., Murakami, H., Narasaki, K., & Hirabayashi, M., 2006, Cryogenics, 46, 149
- Toulemont, Y., private communication, 2005
- Pepi, J. W., & Altshuler, T. L., 1995, Proc. of SPIE, 2543, 201
- Pilbratt, G. T., 2004, Proc. of SPIE, 5487, 401
- Suyama, S., Itoh, Y., Tsuno, K., & Ohno, K., 2005, Proc. of SPIE, 5868, 96
- Yamada, N., & Okaji, M., 2000, High Temp. & High Press., 32, 199

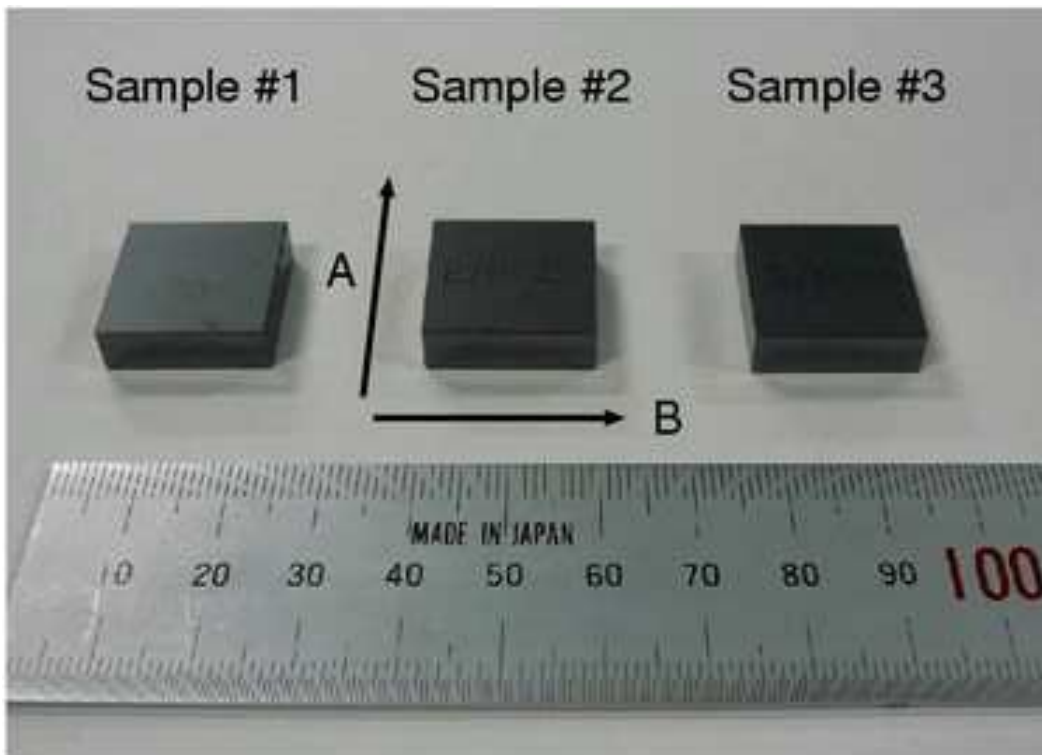


Fig. 1.— Samples measured in this work. The geometry of the samples was  $20.00\text{ mm} \times 20.00\text{ mm} \times 6.0\text{ mm}$ . The surfaces of  $\times 20.00\text{ mm} \times 6.0\text{ mm}$  were polished as described in the text.

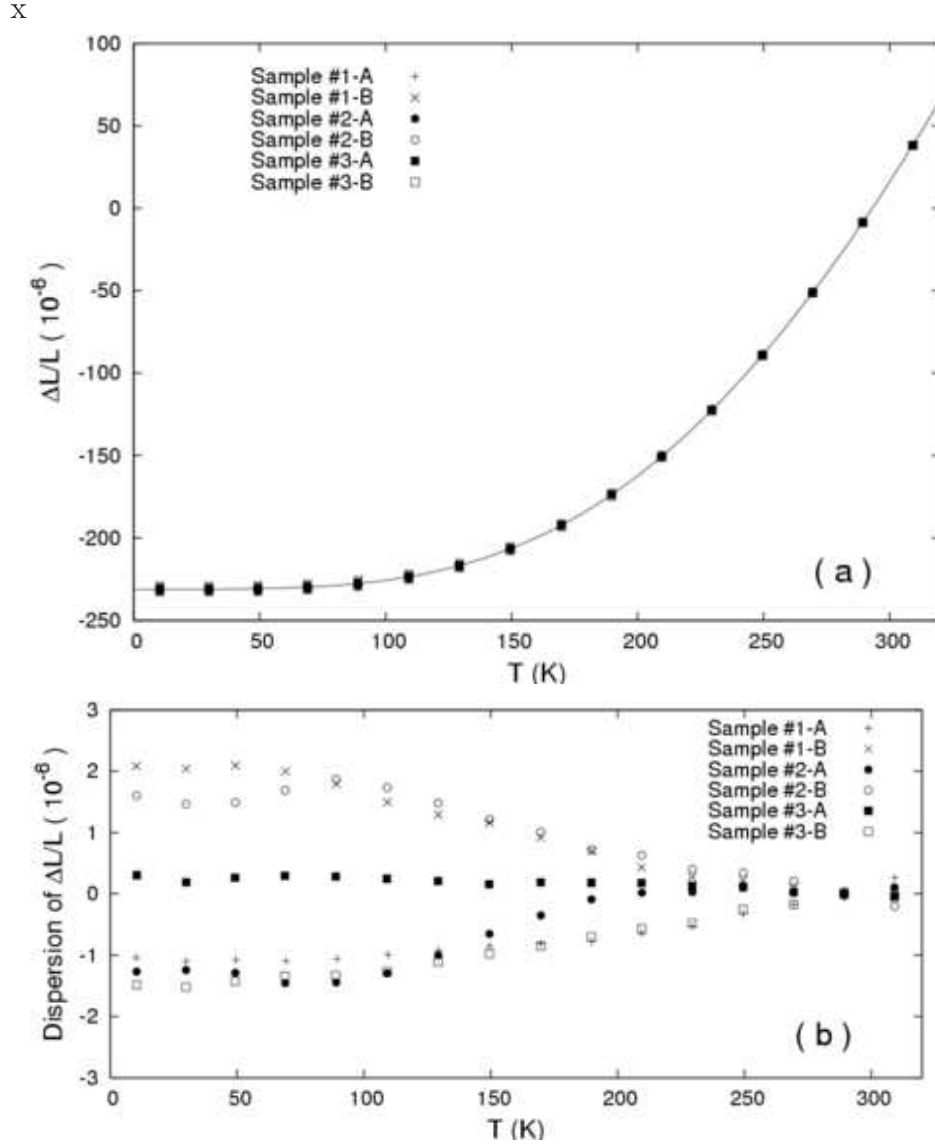


Fig. 2.— Result of the measurements. (a): Thermal expansion data for the direction A and B of the sample #1, #2, and #3. The solid line represents the fitting curve with 8th order polynomial which is expressed by the coefficients presented in table 1. (b): Residual dispersion of the thermal expansion data around the fitting curve.

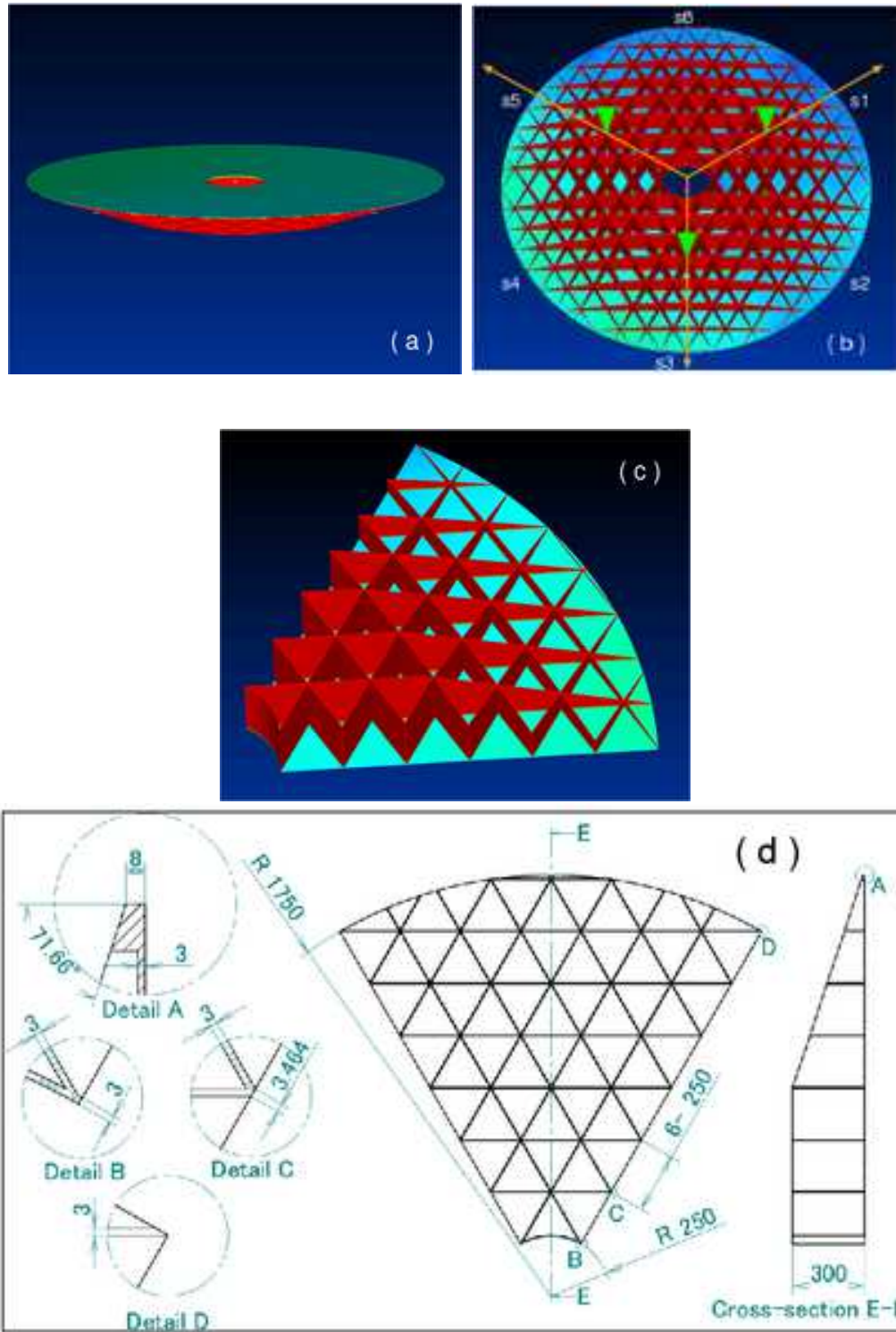


Fig. 3.— The model for the FEM analysis. (a) 3 D view of the model of the whole mirror seen from the reflective side. (b) The same model but seen from the back side of the mirror. Three triangles on the rib indicate points for constraints. All of the three points were constrained in the three lines shown by the arrows. s1 ~ s6 are for ID of the segments (see also figure 4). (c) and (d) shows a 3 D view and the geometry of one segment, respectively.

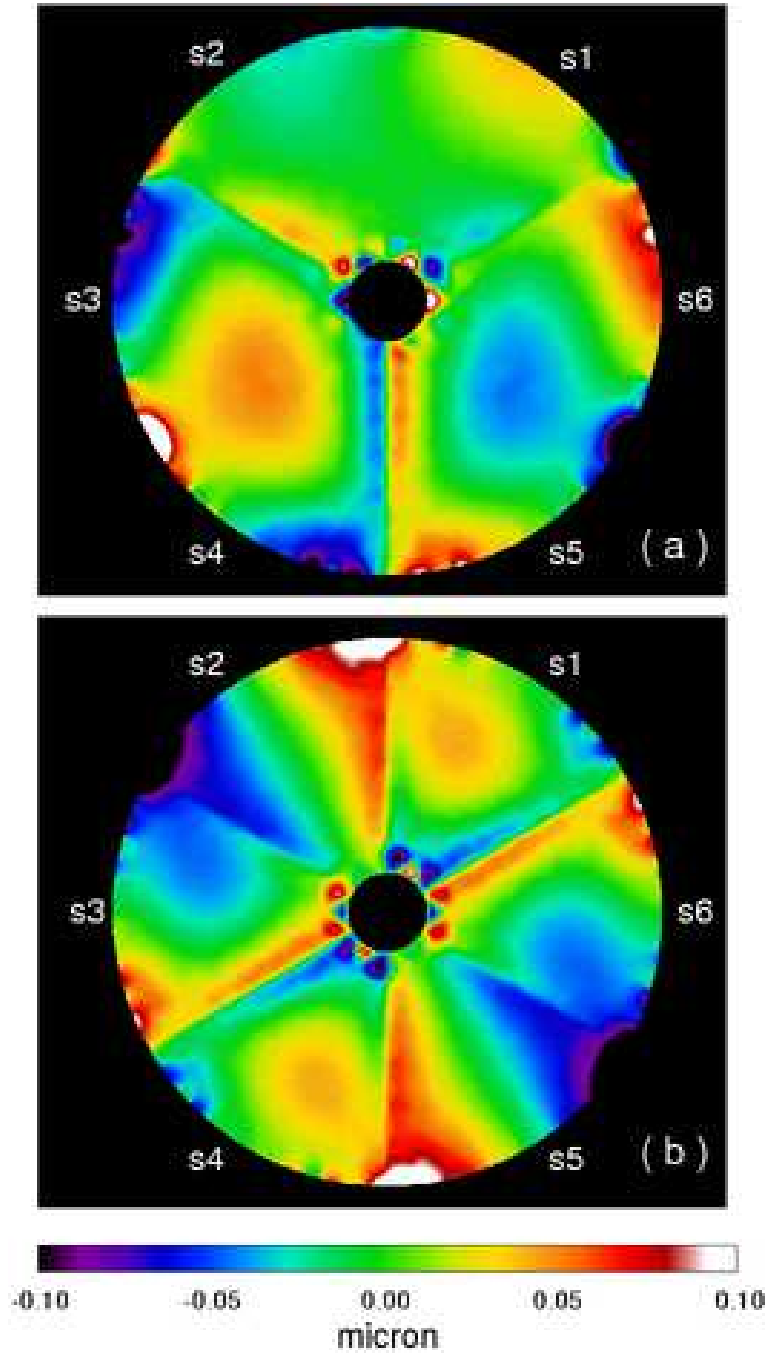


Fig. 4.— The simulated surface deformation by the FEM analysis.  $z$ -direction deformation (i.e., perpendicular to the surface) after tilt correction is shown by color map. (a): The result of the case-I simulation.  $\bar{\alpha}_{\#1}$ ,  $\bar{\alpha}_{\#2}$ , and  $\bar{\alpha}_{\#3}$  were given for the segment s5 and s6, s1 and s2, s3 and s4, respectively. (b): The result of the case-II simulation.  $\bar{\alpha}_{\#1}$ ,  $\bar{\alpha}_{\#2}$ , and  $\bar{\alpha}_{\#3}$  were given for the segment s3 and s6, s2 and s5, s1 and s4, respectively.

Table 1: Coefficients of the 8th order polynomial  $\Delta L/L = \sum_{i=0}^8 a_i T^i$  to represent the typical thermal expansion of SiC-100 below 300 K.

coefficient	value
$a_0$	$+2.43165 \times 10^{-1}$
$a_1$	$-9.25541 \times 10^{-2}$
$a_2$	$+7.38688 \times 10^{-4}$
$a_3$	$+2.44225 \times 10^{-5}$
$a_4$	$+5.68470 \times 10^{-7}$
$a_5$	$+5.94436 \times 10^{-9}$
$a_6$	$-4.04320 \times 10^{-11}$
$a_7$	$+8.70017 \times 10^{-14}$
$a_8$	$-6.64445 \times 10^{-17}$

Table 2: Summary of the measured CTE.

Sample <sup>a</sup>	Direction <sup>b</sup>	$\bar{\alpha}$ (10 <sup>-6</sup> /K) <sup>c</sup>
#1	A	0.820
#1	B	0.809
#2	A	0.821
#2	B	0.811
#3	A	0.815
#3	B	0.822

a, b: #1, #2, and #3 correspond to the sample number and A and B correspond to the direction of the sample for measurement shown in figure 1. xc:  $\Delta L/L$  between 293 K and 10 K.